ELSEVIER

Polymer 42 (2001) 4181–4188

polymer

www.elsevier.nl/locate/polymer

Novel interpenetrating polymer network electrolytes

Xinping Hou, Kok Siong Siow*

Department of Chemistry, The National University of Singapore, 3 Science Drive 3, Singapore 117543, Singapore

Received 1 September 2000; received in revised form 30 October 2000; accepted 7 November 2000

Abstract

A new type of solid polymer electrolyte (SPE) was prepared by sequential interpenetration of cross-linked methoxyoligo (oxyethylene) methacrylate (MOE_nM) and poly(methyl methacrylate) (PMMA). When the interpenetrating polymer networks (IPNs) were swollen with liquid electrolyte solutions, they showed structures that were between the chemically cross-linked gel SPEs and the porous SPE. They could swell/hold much more electrolyte solution than the porous SPE. The electrolytes exhibited ionic conductivities in the order of 10^{-3} S cm^{-1} at 25°C, and could be useful in many practical electrochemical devices. © 2001 Elsevier Science Ltd. All rights reserved.

Keywords: Interpenetrating polymer networks; Micro-phase separation; Ionic conductivity

1. Introduction

Since the discovery by Wright [1] of ionic conduction in polymers containing inorganic salts, and the suggestion by Armand [2] in 1978 that polymer ionic conductors could be used as electrolytes in practical electrochemical devices, much effort has been dedicated to exploring solid polymer electrolytes (SPE) [3–5] for their practical application. Among the various potential applications, the use of SPE in lithium batteries has been most widely studied and is probably the most important and promising application of SPE. In a lithium secondary battery, a polymer electrolyte will function as a separator as well as an electrolyte. The requirements for polymer electrolytes in lithium secondary batteries are, therefore, good mechanical strength (for their function as separators) and favorable electrochemical properties including high ionic conductivity and interfacial compatibility (for their function as electrolytes).

Initial work on polymer electrolytes was mostly based on the complexes of poly(ethylene oxide) (PEO) with inorganic lithium salts. This kind of polymer electrolyte is usually referred to as the first-generation SPE. However, the main drawback of this first-generation SPE is the high degree of crystallization of PEO. This restricts the application of the polymer electrolytes in lithium batteries to temperatures above the melting points of the crystalline PEO, normally around 60°C. At temperatures below the melting points, the conductivities of the polymer electrolytes are just too low to be of practical use, owing to the low segmental movement of polymer chains that restricts the mobility of Li^+ ions.

One of the approaches to overcome the above drawback is to use low molecular weight aprotic plasticizers having high dielectric constant (ε) and low vapor pressure such as propylene carbonate (PC) ($\varepsilon = 64.4$) and ethylene carbonate (EC) ($\varepsilon = 89.6$) [6]. The polymer electrolytes with these plasticizers are known as the second-generation SPE. The plasticizers impart salt-solvating power and high ion mobility to the polymer electrolytes. However, the use of plasticizers tends to decrease the mechanical strength of the electrolytes, particularly at a high degree of plasticization. At the same time, polar solvents are generally reactive towards lithium electrodes, causing lithium batteries with such polymer electrolytes to be plagued often by electrode/electrolyte incompatibilities.

Composite polymer electrolytes with inorganic fillers can be considered the third-generation SPE. Inorganic fillers are used to improve the electrochemical and mechanical characteristics of gel polymer electrolytes (the second-generation SPE) [7–12]. This approach, however, is rather limited because of the small number of inorganic fillers that can be used.

Another approach towards producing polymer electrolytes that have high ionic conductivity (like the gel SPE) and strong mechanical strength would be to use polymers in modified forms. Such modified polymers as copolymers, cross-linked polymers [13–15] and polymer blends [16–17], have shown great potential in overcoming the drawbacks of polymer electrolytes mentioned above.

* Corresponding author. Tel.: +65-8742923; fax: +65-7791691.
E-mail address: chmsks@nus.edu.sg (K.S. Siow).

0032-3861/01/$ - see front matter © 2001 Elsevier Science Ltd. All rights reserved.
PII: S0032-3861(00)00818-1

An interpenetrating polymer network (IPN) is a special kind of polymer blend. An IPN can be defined as a combination of two polymers in network form, one of which is synthesized and/or cross-linked in the immediate presence of the other [18–20]. It can be distinguished from other types of polymer blends in two ways: (i) an IPN swells, but does not dissolve in solvents; and (ii) creep and flow are suppressed in an IPN [21]. An IPN may be made from (i) polymer I, which can complex or hold lithium salts effectively and thus exhibits high ionic conductivity, and (ii) polymer II, which is mechanically and electrochemically stable to lithium electrodes. Such an IPN system would, in principle, make an ideal polymer electrolyte that not only satisfies the dual-function requirement for its use in secondary lithium batteries, but also accommodates the thermal and volumetric changes occasioned by cycling of the lithium anode.

Poly(methyl methacrylate) (PMMA) has been blended with PEO to impart good adhesiveness to solid electrolytes while making them stable to atmospheric moisture [14,22–23]. Scrosati and co-workers [24] showed that PMMA-based electrolytes were either less reactive towards lithium electrode, or able to induce a more favorable passivation film on the electrode surface. Therefore, it is reasonable to consider PMMA as one of the two polymers in an IPN electrolyte system. The present paper reports the synthesis and ionic conductivity study of an IPN electrolyte composed of cross-linked methoxyoligo (oxyethylene) methacrylate (abbreviated as Cr-MOE$_n$M for convenience, where n represents the number of $-CH_2CH_2O-$ units), referred to as polymer I, and PMMA, referred to as polymer II.

2. Experimental

2.1. Materials

Oligo (ethylene glycol) monomethyl ethers (HO–$(CH_2CH_2O)_n$–CH_3) with average molecular weights of 350, 550 and 750 (i.e. $n = 8$, 12 and 16, respectively) were obtained from Fluka. They were azeotropically distilled with benzene to remove residual moisture before use. Methacryloyl chloride (from TCI) was distilled under nitrogen atmosphere to remove the inhibitor immediately before use. Triethylamine (J.T. Baker) was purified by refluxing with anhydrous potassium hydroxide followed by distillation under nitrogen atmosphere. Methanol (J.T. Baker) was dried by refluxing with magnesium powder, and then distilled. Benzene (J.T. Baker) was dried by refluxing with sodium wires followed by distillation. 2,2′-azobisisobutyronitrile (AIBN) (from TCI) was recrystallized from methanol and dried in a vacuum oven at room temperature. Ethylene glycol divinyl ether (Aldrich) and methyl methacrylate (MMA) (Merck) were distilled under reduced pressure to remove the inhibitor immediately before use. High purity (>99%) EC (from Fluka), PC (from Fluka), γ-butyrolactone (γ-BL, from Fluka) and dimethyl carbonate (DMC, from Merck) were used after distillation under reduced or normal pressure. Lithium perchlorate ($LiClO_4$, Fluka) (purity > 97%) and lithium trifluoromethane sulfonate ($LiCF_3SO_3$, Aldrich) were dried at 140°C in a vacuum oven for 24 h before use. Lithium tetrafluoroborate ($LiBF_4$, Aldrich) was used as received. The treated lithium salts and EC, PC, DMC and γ-BL were stored in a dry box filled with purified argon.

2.2. Polymer preparation

Methoxyoligo (oxyethylene) methacrylate (MOE$_n$M, where $n = 8$, 12, 16). They were synthesized following the method of Gramain and Frere [25]. A mixture of 0.10 mol oligo (ethylene glycol) monomethyl ether and 0.12 mol triethylamine in 200 ml of dry benzene was cooled to a temperature below 5°C in an ice-water bath. Methacryloyl chloride (0.11 mol) was added drop-wise into the mixture, stirred and maintained at a temperature below 5°C. When the addition was complete, the reaction mixture was stirred at room temperature overnight. The reaction mixture was filtered off, and the filtrate was washed with warm saturated lithium carbonate solution three times and dried over anhydrous magnesium sulfate overnight in a refrigerator. After the magnesium sulfate was removed, the solvent in the solution was evaporated under reduced pressure at a temperature below 40°C. The residue was then allowed to pass through a silica gel column using chloroform as eluent. After chloroform was completely evaporated under reduced pressure, a pale yellow wax-like product, MOE$_n$M, was obtained. Yield: 74.0%. IR ($cm^{\infty 1}$): 2872 (ν_{C-H}), 1718 ($\nu_{C=O}$), 1637 ($\nu_{C=C}$), 1456 ($\delta_{as,C-H}$), 1350 ($\delta_{a,C-H}$), 1249 ($\nu_{as,C-O-O}$), 1111 ($\nu_{as,C-O-C}$), 1041 ($\nu_{s,C-O-C}$), 948, 854 and 817 ($\varpi_{C=C-H}$). ^{1}H NMR (in $CDCl_3$) δ (ppm): 6.55–5.00 (m, 2H, CH_2=), 4.10–3.90 (m, 2H, $-COOCH_2-$), 3.65–3.25 (m, 4nH, $-(OCH_2CH_2)_n-$), 3.10–3.15 (s, 3H, $-OCH_3$), 1.69 (s, 3H, $=C(CH_3)-$).

Cross-linked poly(methoxyoligo (oxyethylene) methacrylate (Cr-MOE$_n$M). The reaction mixtures were prepared by mixing the methoxyoligo (oxyethylene) methacrylate (MOE$_n$M), ethylene glycol divinyl ether (cross-linker, 5, 10, and 20 wt% of MOE$_n$M, respectively) and 2,2-dimethoxy-2-phenylacetophenone (DMPA, initiator, 1 mol% of total monomers). The mixtures were cast into Teflon molders. They were then irradiated with UV light (10 mW cm^{-2}, 365 nm) for 30 min in N_2 atmosphere. To estimate the gel fraction of the network polymers produced, the films (~0.2 mm in thickness) were extracted in methanol for 8 h using Soxhlet's extractors and then dried in a vacuum oven at 100°C for 48 h to remove the solvent. Their IR spectra showed that there was no peak at ~1640 cm^{-1}, indicating that the unreacted monomers had been extracted completely. The gel fraction was calculated from the following equation:

$$\text{Gel fraction} = (A/B) \times 100\% \quad (1)$$

where A and B are the weights of the network polymers after and before extraction, respectively.

Interpenetrating polymer networks Cr-MOE$_n$M (I)/ PMMA (II). Films of cross-linked MOE$_n$M were soaked in a mixture consisting of MMA, 5 wt% of 1,4-butanediol dimethacrylate (a common cross-linking agent for PMMA) and 1 mol% AIBN (initiator). The ratio of Cr-MOE$_n$M to PMMA was controlled by varying the duration for which the films were left soaking in the mixture. The ratios were determined by weighing the films before and after soaking. The films (after soaking) were then polymerized in N_2 atmosphere at 60, 80 and 90°C for 24 h, respectively. The IPN films thus obtained were subsequently extracted with methanol for 8 h and dried in a vacuum oven at 100°C for at least 48 h before they were stored in a dry box filled with argon. The IR spectra of the IPN films were taken with a BIO-RAD FT-IR spectrophotometer. No peak at $\sim$1640 cm^{-1} was observed. The gel fraction was calculated according to Eq. (1).

To examine their swelling behavior, dry IPN films (approximate dimensions: 10 mm × 10 mm × 0.2 mm) with accurately known weights were immersed in organic solvents: EC–DMC (1:1 by volume), γ-BL and EC–PC (1:1 by volume), and liquid electrolyte solutions: 1 M $LiClO_4$ in EC–DMC, 1 M $LiBF_4$ in γ-BL and 1 M $LiCF_3SO_3$ in EC–PC. The swelling processes were carried out in a dry box filled with purified argon at about 30°C. The IPN films were taken out from the solvent or liquid electrolyte solutions at different times to determine the solvent or solution contents (SC) in the samples defined as:

$$\mathrm{SC}\ (\%) = (W_s - W_0)/W_s \times 100\% \quad (2)$$

where W_0 and W_s are the weights of the IPN samples before and after swelling.

2.3. Measurements

Thermal analysis. Thermal analysis of IPN films was carried out using a Universal TA Instrument DSC 2960 Thermal Analyzer (DuPont) under nitrogen atmosphere at a heating rate of 10°C min^{-1} from −150 to 150°C. The glass transition temperature (T_g) was taken as the temperature of the midpoint of the baseline shift. The melting point (T_m) was taken as the peak temperature of the endothermic peak. The crystallinity (χ_c) was estimated from the ratio of the experimentally determined ΔH_m to the value of 213 J g^{-1} reported for the enthalpy of melting of 100% crystalline PEO [26]. The samples for thermal analysis were sealed in aluminum pans in the dry box to avoid any moisture, which might affect the thermal properties of the samples.

Morphology observation. The IPN films were first frozen in liquid nitrogen and fractured mechanically. They were then vacuum-dried at room temperature for 24 h before they were coated with gold using a BAL-TEC sputter coater SCD005. For the samples swollen with liquid electrolyte solutions (1 M $LiClO_4$ in EC–DMC, 1 M $LiBF_4$ in γ-BL and 1 M $LiCF_3SO_3$ in EC–PC), freeze-drying was carried out to ensure that no morphology changes took place when the electrolyte solutions were removed. The morphologies of cross-section of gold-coated samples were examined with a Philips XL30 scanning electron microscope (SEM).

Conductivity measurements. Ionic conductivities of the IPN films after equilibrium swelling with liquid electrolyte solutions of lithium salts were determined from the ac impedance spectra taken from 10 to 80°C for cells assembled by sandwiching the films between two stainless steel (SS) blocking electrodes of diameter 12.86 mm. An EG&G Potentiostat/Galvanostat Model 273A coupled with a Lock-In Amplifier (5210) was employed for the measurements. During the measurements, the surface of the cells was connected to the ground to eliminate the effect of surface current. The data were collected over a frequency range from 100 kHz to 10 Hz. 5 mV ac amplitude was applied during the measurement. A thermostat bath with 0.1°C precision was used to control the temperature. Ionic conductivities were calculated from the bulk resistance obtained from the impedance spectra:

$$\sigma = L/(RA) \quad (3)$$

where R is the bulk resistance, A the area of the electrode, and L the thickness of sample, which can be obtained from the difference in end-to-end distance of the two electrodes with and without a sample in between them. Because moisture can affect the performance of cells substantially, especially the ionic conductivity of the electrolytes in our study, the whole installation procedure of the cell was carried out in a dry box. The cell was sealed tightly before being taken out of the dry box for measurements. Each sample was equilibrated at the experimental temperature for 30 min before measurements.

3. Results and discussion

3.1. Synthesis of IPNs

The gel fraction values of cross-linked MOE$_n$M networks and Cr-MOE$_n$M/PMMA IPNs are shown in Table 1. The data show that the gel fraction values of cross-linked MOE$_n$M networks are all above 95%. It is worth noting that the soluble fraction in the polymer networks can affect not only the extent to which the networks may be swollen (with the mixture consisting of MMA, 5 wt% of 1,4-butanediol dimethacrylate (cross-linker) and 1 mol% AIBN (initiator)), but also the mechanical strength and ionic conductivity of the networks. Since there was no difference in gel fraction values between the polymer networks with different contents of EGDE and since ionic mobility of lithium salt usually decreases with increase in degree of cross-linking (i.e. with increasing weight percentage of EGDE in this case), we chose to use the polymer network cross-linking with 10 wt% of EGDE in our studies.

Table 1
The gel fraction of polymer network I and IPN films

Polymer abbreviation	EGDE[a] amount (wt% of MOE_nM)	PMMA content (wt% of IPN film)	Gel fraction in network polymers or IPN films (wt%)
Cr-MOE_8M	5	0	97.6
	10	0	98.0
	20	0	98.5
Cr-$MOE_{12}M$	5	0	96.8
	10	0	97.3
	20	0	97.0
Cr-$MOE_{16}M$	5	0	95.7
	10	0	96.3
	20	0	96.5
Cr-$MOE_{12}M$/10PMMA	–	10	98.1
Cr-$MOE_{12}M$/25PMMA	–	25	97.5
Cr-$MOE_{12}M$/35PMMA	–	35	97.0
Cr-$MOE_{12}M$/50PMMA	–	50	96.8
Cr-$MOE_{12}M$/60PMMA	–	60	96.1

[a] Ethylene glycol divinyl ether (cross-linker).

This network has also many more desirable mechanical properties compared to the networks with 5 or 20 wt% of EGDE. For the IPNs, the gel fraction values are also all around 97%. Fig. 1 shows the IR spectra of $MOE_{12}M$, cross-linked $MOE_{12}M$ network and the IPN (Cr-$MOE_{12}M$/PMMA). It is clear that the peak at about 1640 cm^{-1} for carbon–carbon double bonds in the monomer $MOE_{12}M$ does not appear in the infrared spectra of the cross-linked $MOE_{12}M$ network and the IPN, indicating that there is no monomer residue left in the networks after the extraction.

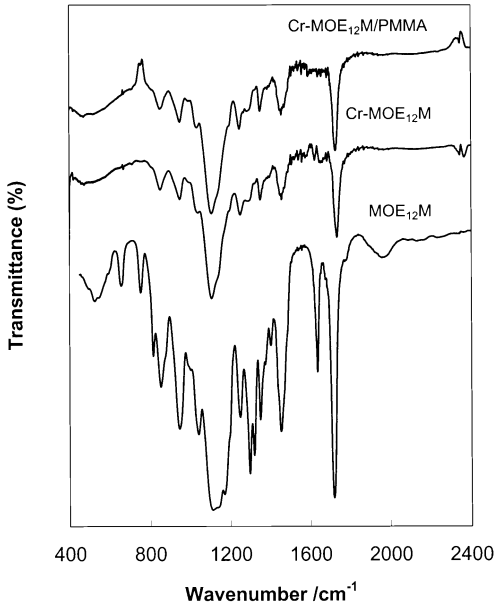

Fig. 1. Infrared spectra of a typical Cr-MOE_nM/PMMA film along with Cr-MOE_nM and MOE_nM.

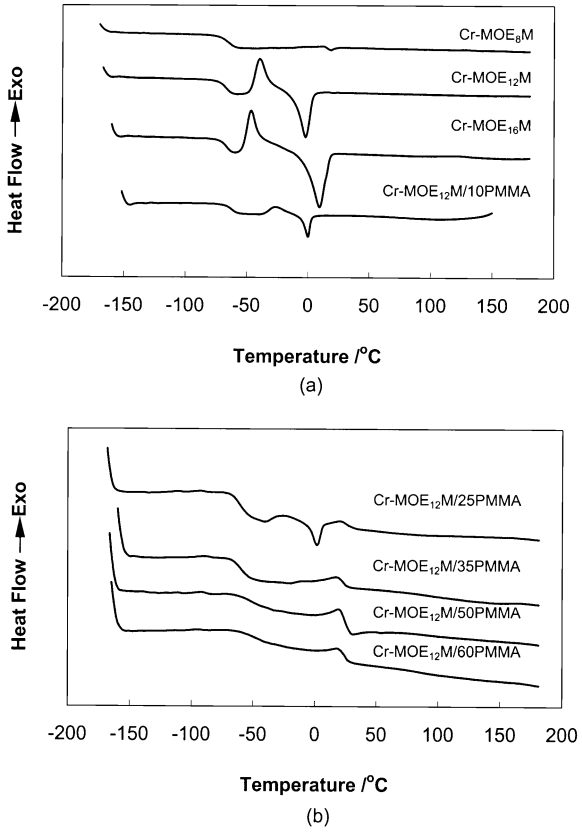

Fig. 2. DSC curves of the Cr-MOE_nM with different lengths of oligo (oxyethylene) side chain and the Cr-$MOE_{12}M$/PMMA networks with different PMMA contents.

3.2. Thermal properties

Fig. 2 shows the DSC curves of the cross-linked MOE_nM and the interpenetrating networks. The T_g, T_m, ΔH_m and degree of crystallinity (χ_c) of these networks are summarized in Table 2. For the cross-linked MOE_nM networks, their melting points (T_m, from −1.2°C (for $n = 12$) to 9.6°C (for $n = 16$)) and degrees of crystallinity (χ_c, from 9.2% (for $n = 12$) to 16.5% (for $n = 16$)) both increase with increasing length of the oligo (oxyethylene) side chain (i.e. the n values). It is to be noted that cross-linking inhibits the crystallization of oligo (oxyethylene) side chains, as can be seen from their values of χ_c, which are much lower than those of the corresponding linear PEO [26]. The glass transition temperatures (T_g) of the cross-linked MOE_nM networks (with different n values) are all around −65°C. It is noted that oligo-PEO also shows a glass transition temperature around −65°C. It is reasonable, therefore, to assign the glass transition temperature of the cross-linked MOE_nM at −65°C, as being due to the glass transition of the oligo (oxyethylene) side chains.

All the Cr-$MOE_{12}M$/PMMA IPNs have a glass transition (referred to as T_{g1}) at temperatures below 0°C. As in the case of Cr-$MOE_{12}M$, this glass transition temperature can be assigned to the contribution of oligo (oxyethylene) side

Table 2
DSC data of the synthesized polymer networks along with the crystallinity values (χ_c)

Polymer networks	T_{g1} (°C)	T_{g2} (°C)	T_m (°C)	ΔH_m (J g^{-1})	χ_c (%)
Cr-MOE$_8$M	−64.7	–	–	–	–
Cr-MOE$_{12}$M	−66.8	–	−1.2	18.7	9.2
Cr-MOE$_{16}$M	−66.3	–	9.6	33.5	16.5
Cr-MOE$_{12}$M/10PMMA	−64.3	–	1.1	0.22	0.1
Cr-MOE$_{12}$M/25PMMA	−61.7	–	−1.6	0.02	0.01
Cr-MOE$_{12}$M/35PMMA	−59.5	25.6	–	–	–
Cr-MOE$_{12}$M/50PMMA	−50.5	24.8	–	–	–
Cr-MOE$_{12}$M/60PMMA	−41.7	24.1	–	–	–

chains. The values of T_{g1}, however, increase with increasing content of PMMA in the Cr-MOE$_{12}$M/PMMA IPNs. For the IPNs with more than 25 wt% PMMA, a second glass transition (referred to as T_{g2}) also appears around 25°C.

In the sequential IPNs, in general, the phase domain size of polymer II (PMMA in our case) depends on a number of factors, including: the cross-linking density of polymer I (Cr-MOE$_n$M in our case), the volume fraction of each polymer, the interfacial tension and the temperature. For our IPN system, when the PMMA content is not more than 25 wt%, there is only one T_g (i.e. T_{g1}) at a temperature below 0°C, which is due to the contribution of oligo (oxyethylene) side chains. This reflects that there is a continuous phase of Cr-MOE$_n$M in the Cr-MOE$_{12}$M/PMMA IPNs with less than 25 wt% PMMA. The phase domain structure of PMMA in these Cr-MOE$_{12}$M/PMMA IPNs is not continuous and is dispersed in the continuous Cr-MOE$_{12}$M phase. For the IPNs with more than 25 wt% PMMA content, two glass transitions were observed: T_{g1} owing to the Cr-MOE$_{12}$M phase, and T_{g2} owing to the PMMA phase. This reflects that the PMMA phase also becomes continuous now when its content in IPNs is more than 25 wt%. It is worth noting that T_{g2} (~25°C) is fairly below the glass transition of ordinary PMMA (80–100°C). This can be explained as being due to the effects of synergisms, which result frequently from interpenetration. These synergisms usually make the phase properties of each component deviate from those without synergisms.

It is also noted that T_{g1} increases from −64.3 to −41.7°C with increasing PMMA content. For our Cr-MOE$_{12}$M/PMMA IPNs, the Cr-MOE$_{12}$M was swollen with MMA monomer mixtures, which were then polymerized with cross-linking. This is a process of chemical network growth with diffusion-controlled dynamics of the monomers and network units [27]. The amount of MMA socked in Cr-MOE$_{12}$M and the time and temperature of socking will affect the phase structure of Cr-MOE$_{12}$M, especially its volume fraction. The more the PMMA content in IPNs, the stronger will be the chemical interactions and network entanglements arising from interpenetration [21], and the more obvious the change of T_{g1}.

The dispersion of PMMA in the Cr-MOE$_{12}$M phase also decreases the crystallinity in Cr-MOE$_{12}$M, as can be seen from the χ_c values (see Table 2, from 16.5% with no PMMA to 0.1 and 0.01% when PMMA content is 10 and 25 wt%). When the PMMA content in IPNs reaches 35 wt%, the crystallinity of oligo (oxyethylene) side chain in the Cr-MOE$_{12}$M phase is eliminated completely.

3.3. Swelling properties

Figs. 3–5 show the swelling behavior of the various interpenetrating networks. It can be seen clearly from Figs. 3 and 4 that the SC of IPNs in both EC–DMC and liquid electrolyte solution of 1 M $LiClO_4$ in EC–DMC increases with decreasing PMMA content. This can be attributed to the interaction of EC–DMC and the liquid electrolyte solution with Cr-MOE$_{12}$M phase. The oligo (oxyethylene) side chain in cross-linked MOE$_{12}$M can interact with EC–DMC and lithium salts, while the cross-linked PMMA phase will not interact with EC–DMC or the liquid electrolyte solution [28].

For IPNs with 25 wt% PMMA, the SC for 1 M $LiCF_3SO_3$ in EC–PC is higher than that for 1 M $LiClO_4$ in EC–DMC

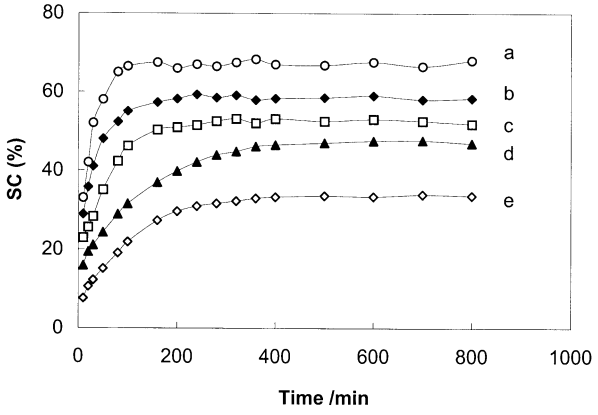

Fig. 3. Solvent/solution content of EC–DMC in Cr-MOE$_{12}$M/PMMA networks with different PMMA content: (a) 10, (b) 25, (c) 35, (d) 50, and (e) 60 wt%.

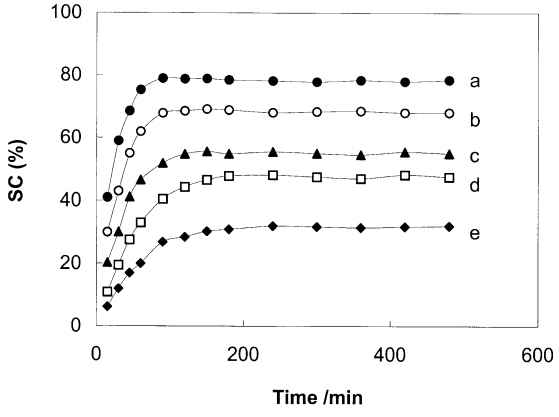

Fig. 4. Solvent/solution content of 1 M $LiClO_4$ in EC–DMC in Cr-MOE$_{12}$M/PMMA networks with different PMMA content: (a) 10, (b) 25, (c) 35, (d) 50, and (e) 60 wt%.

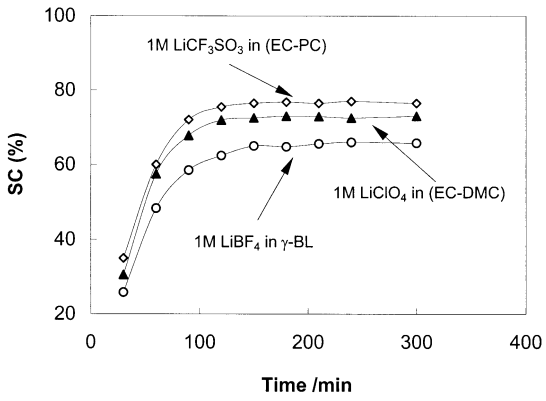

Fig. 5. Solvent/solution content of different liquid electrolyte solutions in Cr-MOE_{12}M/PMMA networks with 25 wt% PMMA.

and 1 M $LiBF_4$ in γ-BL, as can be seen from Fig. 5. This may be due to the increase in the polarity of the solvent used, which is favorable for its percolation in polar IPNs, especially the Cr-MOE_{12}M phase component. The polarity of EC and PC are higher than DMC and γ-BL. The polarity of the solvent mixture solvent EC–DMC should also be slightly higher than that of γ-BL. The SC for 1 M $LiClO_4$ in EC–DMC is therefore still slightly higher than that of 1 M $LiBF_4$ in γ-BL.

3.4. Morphology

Fig. 6 shows the SEM images of the cross-section of Cr-MOE_{12}M/PMMA interpenetrating networks with different compositions. For the image of pure Cr-MOE_{12}M (see Fig. 6(a)), some fine cracks (10–50 nm) were observed clearly, showing that there is crystalline structure in the networks, which appeared as cracks because of shrinking during the cross-linking. There are also some veins, which belong to the pattern of tear fracture. The morphology of IPN with 10 wt% of PMMA was much smoother compared to that of pure Cr-MOE_{12}M though very few fine cracks could still be recognized (see Fig. 6(b)). When the PMMA component increased to 25 wt% (see Fig. 6(c)), the IPN had an irregular wavelike uneven appearance, owing to the interpenetration between the two networks. At the same time, hardly any cracks were observed in Fig. 6(c), indicating that the crystallization had been eliminated by interpenetration. After swelling of the liquid electrolyte solution, the IPN with 25 wt% PMMA showed a porous structure with a micro-phase separation (see Fig. 6(d)). Such a structure lies between the chemically cross-linked gel SPEs and the porous SPEs [29]. It has a homogeneous macro-structure (like the gelled SPE), physically preventing separation of the matrix polymer and the electrolyte solution. On the other

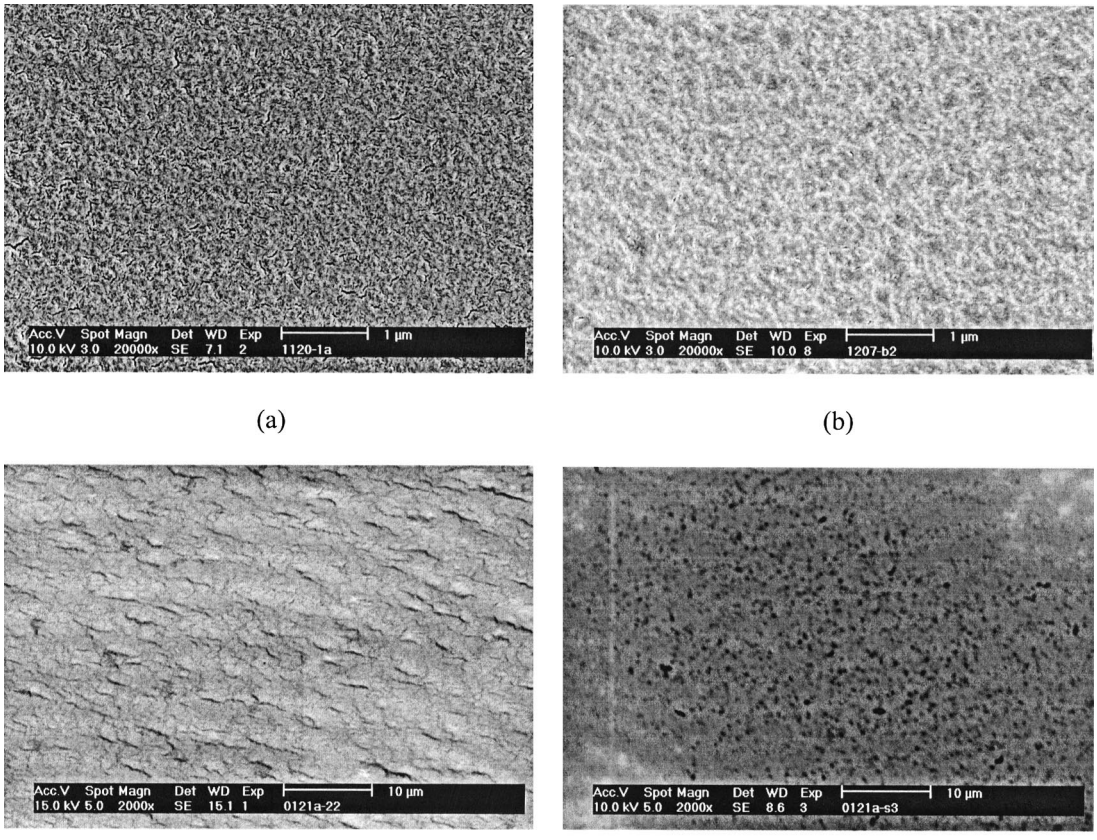

Fig. 6. SEM images of the cross-sections of Cr-MOE_{12}M/PMMA IPN films with different compositions.

hand, it maintains sufficient osmosis pressure to be leak-proof in practice because of the interaction of the oligo (oxyethylene) side chain of Cr-MOE$_n$M with the liquid electrolyte solution and the strong swelling capability of IPN (like the porous SPE) [30,31].

Patterson and co-workers [32] and Prins and co-workers [33] presented a theoretical analysis of equilibrium swelling of a network in a single solvent. This study led to the prediction that a swollen network in equilibrium with pure solvent may undergo a phase transition into two phases with different degrees of swelling. Later experimental work [34,35] has verified the prediction. In our IPN films, the micro-phase separation takes place because of the different degree of swelling of the two components (Cr-MOE$_n$M and PMMA).

3.5. Ionic conductivity

The IPN films exhibit ionic conduction after swelling liquid electrolyte solution such as 1 M $LiClO_4$ in EC–DMC, 1 M $LiCF_3SO_3$ in EC–PC and 1 M $LiBF_4$ in γ-BL. Fig. 7 shows the temperature dependence of ionic conductivities of the Cr-MOE$_{12}$M/PMMA IPNs with different amounts of PMMA after swelling 1 M $LiClO_4$ in EC–DMC for 4 h. It is clear that, after swelling 1 M $LiClO_4$ in EC–DMC for 4 h, Cr-MOE$_{12}$M/0PMMA (0PMMA indicate a 0% of PMMA in the sample), Cr-MOE$_{12}$M/10PMMA and Cr-MOE$_{12}$M/25PMMA have much higher ionic conductivities than the IPN films with 35 wt% PMMA and above. This can be explained by the DSC results and the morphology of the IPNs. When PMMA reaches 35 wt%, the cross-linked PMMA phase will be continuous in IPNs as can be seen clearly from DSC curves where the second T_g (T_{g2})

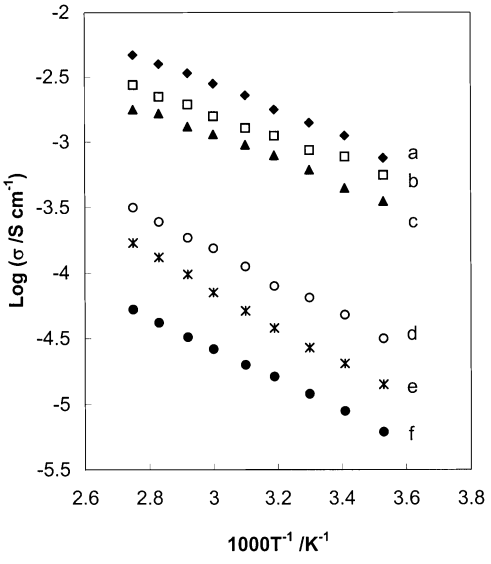

Fig. 7. The temperature dependence of ionic conductivities of the Cr-MOE$_{12}$M/PMMA IPN films with different amount of PMMA after swelling 1 M $LiClO_4$ in EC–DMC for 4 h: (a) 0, (b) 10, (c) 25, (d) 35, (e) 50, and (f) 60 wt% PMMA.

appeared and got more and more obvious with the increase of PMMA. The IPNs also got more and more tough and lost their elasticity when PMMA reached 50 wt%. The capability of absorbing liquid electrolyte solutions decreased a lot because of the decrease of volume fraction of the Cr-MOE$_{12}$M that provided moving channels for lithium ions. On the other hand, when the PMMA component was 10 wt% and less, the IPNs became soft after absorbing liquid electrolyte solutions because of the strong interaction between electrolyte solutions and oligo (oxyethylene) side chains. The mechanical strength decreased, and the IPNs had to be handled very carefully, which is not favorable for practical use.

It is noted that all the conduction behaviors obey Arrhenius equation:

$$\sigma = A \exp[-E_a/RT] \quad (4)$$

where A is a pre-exponential factor, E the activation energy and T the temperature in Kelvin. This is different from that of PEO–PMMA matrix system [13,36], which showed VTF (Vogel–Tamman–Fulcher) behavior:

$$\sigma = AT^{-0.5} \exp[-B/(T - T_0)] \quad (5)$$

where B is a pseudoactivation energy for ionic conductivity in Kelvin, A a pre-exponential factor that is proportional to the number of charge carriers, and T_0 (in Kelvin) a quasi-equilibrium glass transition temperature, which has been reported to be 30–50°C lower than T_g for many polymer electrolyte systems [37]. It can be assigned to the different preparation methods and the morphology of the two systems. In the PEO–PMMA matrix system, PEO-grafted poly(methylmethacrylate) (PEO–PMMA) was cured with lithium salt by poly(ethylene glycol) dimethacrylate (PED) through photo-induced radical polymerization. The ionic conduction was related to the movement of PEO chains closely. So they obey the VTF equation. In our system, though the segmental movement is also important (which is why we chose Cr-MOE$_n$M as one of our components), the absorption ability of the polymer matrix for the liquid electrolyte solution is even more important to ensure the polymer matrix can swell and hold as much as possible liquid electrolyte solutions while maintaining good mechanical strength. The conduction here depended much more on the channels the polymer networks provided than the segmental movement of the polymers. Therefore, the conduction behavior obeys the Arrhenius equation. Just as we mentioned above, our system is a micro-phase separation-type SPE, which lies between the chemical cross-linking gel SPE (like the PEO–PMMA matrix system) and the porous SPE (like P (VDF–HFP) system) developed by Gozdz et al. [30].

4. Conclusions

A new type of cross-linked methoxyoligo (oxyethylene)

methacrylate (Cr-MOE$_n$M)/PMMA interpenetrating polymer network (IPN) electrolyte was synthesized by swelling the IPNs with liquid electrolyte solutions. Thermal analysis showed that interpenetration eliminated the crystallization in Cr-MOE$_n$M. The IPNs with 35 wt% PMMA and above had two T_gs, showing that phase separation had taken place in them. The morphology of the IPNs was studied with SEM, confirming the DSC results. It is also shown that our system is a micro-phase separation-type SPE, which lies between the chemical cross-linked gel SPE and the porous SPE. It can swell more liquid electrolyte solution than the ordinary porous SPE because of the strong interaction of electrolyte solutions and one of the interpenetrating components. The ionic conduction obeys the Arrhenius equation. The ionic conductivities are about 10^{-3} S cm^{-1} at room temperature. These ionic conductive materials can be further developed as SPE for potential applications in many electrochemical devices.

Acknowledgements

The authors are grateful to the National University of Singapore for a research grant for this work.

References

[1] Wright PV. Br Polym J 1975;7:319.
[2] Armand MB, Chabago JM, Dulcot M. Extended Abstracts: The 2nd International Conference on Solid Electrolytes, St. Andrews, Scotland, September 1978.
[3] MacCallum JR, Vincent CA, editors. Polymer electrolyte reviews, vols. 1 and 2. New York/London: Elsevier, 1987–1989.
[4] Gray FM, editor. Solid polymer electrolytes: fundamentals and technological applications. New York: VCH, 1991.
[5] Gray FM. Polymer electrolytes. Cambridge: The Royal Society of Chemistry, 1997.
[6] Dominey LA. In: Pistoia G, editor. Lithium batteries — new materials, developments and perspectives. Amsterdam: Elsevier, 1994.
[7] Wieczorek W, Such K, Wycislik H, Plocharski J. Solid State Ionics 1989;36:225.
[8] Croce F, Scrosati B, Mariotto G. Chem Mater 1992;4:1134–6.
[9] Khan SA, Baker GL, Colson S. Chem Mater 1994;6:2359.
[10] Borghini MC, Passerini M, Scrosati B. J Electrochem Soc 1995;142:2118.
[11] Appetecchi GB, Dautzenberg G, Scrosati B. J Electrochem Soc 1996;143:6.
[12] Hou J, Baker GL. Chem Mater 1998;10:3311–8.
[13] Morita M, Fukumasa T, Motoda M, Tsutsumi H, Matsuda Y. J Electrochem Soc 1990;137(11):3401–4.
[14] Mani R, Mani T, Stevens JR. J Polym Sci Part A Polym Chem 1992;30:2025–31.
[15] Li D, Hu CP, Ying SK. Solid State Ionics 1994;72:172.
[16] Rhoo HJ, Kim HT, Park JK, Huang TS. Electrochim Acta 1997; 42(10):1571.
[17] Chu PP, Jen HP, Lo FR, Lang CL. Macromolecules 1999;32:4738–40.
[18] Lipatov YS, Sergeva LM. Interpenetrating polymeric networks. Kiev: Naukova Dumka, 1979.
[19] Klempner D, Frisch DC, editors. Polymer alloys, vol. II. New York: Plenum Press, 1980.
[20] Sperling LH. Interpenetrating polymeric networks and related materials. New York: Plenum Press, 1981.
[21] Kim SC, Sperling LH, editors. IPNs around the world — science and engineering. New York: Wiley, 1997.
[22] Mani T, Stevens JR. Polymer 1992;33(4):834–7.
[23] Mani T, Mani R, Stevens JR. Solid State Ionics 1993;60:113–7.
[24] Ostrovskii D, Torell LM, Appetecchi GB, Scrosati B. Solid State Ionics 1998;106:19–24.
[25] Gramain P, Frere Y. Polym Commun 1986;27:16.
[26] Li X, Hsu SL. J Polym Sci Part B Polym Phys 1984;22:1331.
[27] Frisch HL, Du Y, Schulz M. Polymer networks — principles of their formation, structure and properties. London: Blackie, 1998.
[28] Cazzanelli E, Mariotto G, Appetecchi GB, Croce F, Scrosati B. Electrochim Acta 1995;40(13–14):2379–82.
[29] Murata K, Izuchi S, Yoshihisa Y. Electrochim Acta 2000;45:1501–8.
[30] Gozdz AS, Tarascon JM, Schmutz CN, Warren PC, Gebizlioglu OS, Shokoohi F. Proceedings of the 10th Annual Battery Conference on Applications and Advances, 1995. p. 301.
[31] Xu W, Siow K, Gao Z, Lee S, Chow P, Gan L. Langmuir 1999;15:4812–9.
[32] Dusek K, Patterson D. J Polym Sci 1968;A2(6):1209.
[33] Dusek K, Prins W. Adv Polym Sci 1969;6:1.
[34] Tanaka T. Phys Rev Lett 1978;40:820.
[35] Ilavsky M. Macromolecules 1982;15:782.
[36] Morita M, Araki F, Kashiwamura K, Yoshimoto N, Ishikawa M. Electrochim Acta 2000;45(8–9):1335–40.
[37] Adam G, Gibbs JH. J Chem Phys 1965;43:139.